



## Photodynamic inactivation of *Staphylococcus aureus* using low symmetrically substituted phthalocyanines supported on a polystyrene polymer fiber

Nkosiphile Masilela<sup>a</sup>, Phumelele Kleyi<sup>a</sup>, Zenixole Tshentu<sup>a</sup>, Georgios Priniotakis<sup>b</sup>, Philippe Westbroek<sup>c</sup>, Tebello Nyokong<sup>a,\*</sup>

<sup>a</sup>Department of Chemistry, Rhodes University, Grahamstown 6140, South Africa

<sup>b</sup>Technological Educational Institute of Piraeus, Textile Engineering Department, Petrou Ralli & Thevon 250, Aegaleo 12244, Athens, Greece

<sup>c</sup>Ghent University, Department of Textiles, Technologiepark 907, B-9052 Gent, Belgium

### ARTICLE INFO

#### Article history:

Received 13 July 2012

Received in revised form

30 September 2012

Accepted 2 October 2012

Available online 23 October 2012

#### Keywords:

Low symmetry phthalocyanines

Germanium

Titanium

Antimicrobial

Photodynamic therapy

Electrospun fiber

### ABSTRACT

This work reports on the antimicrobial photo-activities of a series of low symmetrically substituted phthalocyanine complexes in solution and in a fiber matrix. Phthalocyanine complexes were successfully electrospun into a polystyrene polymer. The fiber diameter ranged from 240 nm to 390 nm in average. The modified polymer fiber showed successful singlet oxygen production with the Ge monocarboxy phthalocyanine modified fiber giving the highest singlet oxygen quantum yield value of 0.46 due to lack of aggregation when in the polymer. All the unsymmetrically substituted complexes showed antimicrobial activity towards *S. Aureus* under illumination with visible light. The symmetrical ZnPc and ZnTPCPC showed no activity under illumination with light in the fiber matrix due to low singlet oxygen production.

© 2012 Elsevier Ltd. All rights reserved.

### 1. Introduction

Phthalocyanines (Pcs) continue to receive attention for applications in a variety of scientific fields due to their unique physico-chemical properties that arise from their aromatic structure [1,2]. A number of Pcs show potential as photosensitizers for photodynamic therapy (PDT) of cancer [3–7]. PDT has been considered as a low-cost, non-invasive and a gentle procedure for treatment of various tumors [8]. PDT may be applied with high efficiency for inactivation of pathogenic microorganisms which are resistant to antibiotics [9], hence this work reports on a series of Pcs for the inactivation of *Staphylococcus aureus* bacteria. Pcs show high efficiency of generating reactive oxygen species, have low dark toxicity and can easily be chemically modified [10]. Previous reports have shown that introducing diamagnetic metals such as Zn, Si, Al, Ga and In into the cavity of the Pc ring results in enhanced triplet state parameters (triplet quantum yields and lifetimes) and high singlet oxygen quantum yields [11–14].

The use of symmetrically substituted Pcs as photosensitizers for photodynamic therapy is well established, however these complexes show low substrate binding selectivities [15]. It has also been reported that decreasing the symmetry of phthalocyanines improves the singlet oxygen quantum values [16], hence in this work, low symmetry Pc complexes **1–5**, symmetrical complex **6** and unsubstituted zinc phthalocyanine (Fig. 1 and Schemes 1 and 2) are reported for the inactivation of *S. aureus* bacteria. Cosimelli et al. reported that low symmetry zinc phthalocyanine (in solution) showed photo-inhibition of *Candida albicans* [17]. We have recently reported on the inactivation of *S. aureus* using phthalocyanines in solution and in the presence of nanoparticles [18]. The use of supports for phthalocyanines during the inactivation of bacteria is preferred since it allows for recyclability. The use of unsubstituted zinc phthalocyanine (ZnPc) embedded in electrospun polyurethane fibers has been reported by Mossinger et al. for the inactivation of *Escherichia coli* [19]. In this work, low symmetrically substituted phthalocyanine complexes embedded in electrospun polystyrene (PS) polymer material are used for the inactivation of *S. aureus* bacteria, a gram positive and drug resistant bacteria. We investigate the photochemical behavior of MPc-PS fiber composite and their antimicrobial activity towards *S. aureus*. The effects of asymmetrical versus symmetrical substitution on the phthalocyanines are

\* Corresponding author. Tel.: +27 46 6038260; fax: +27 46 6225109.  
E-mail address: [t.nyokong@ru.ac.za](mailto:t.nyokong@ru.ac.za) (T. Nyokong).

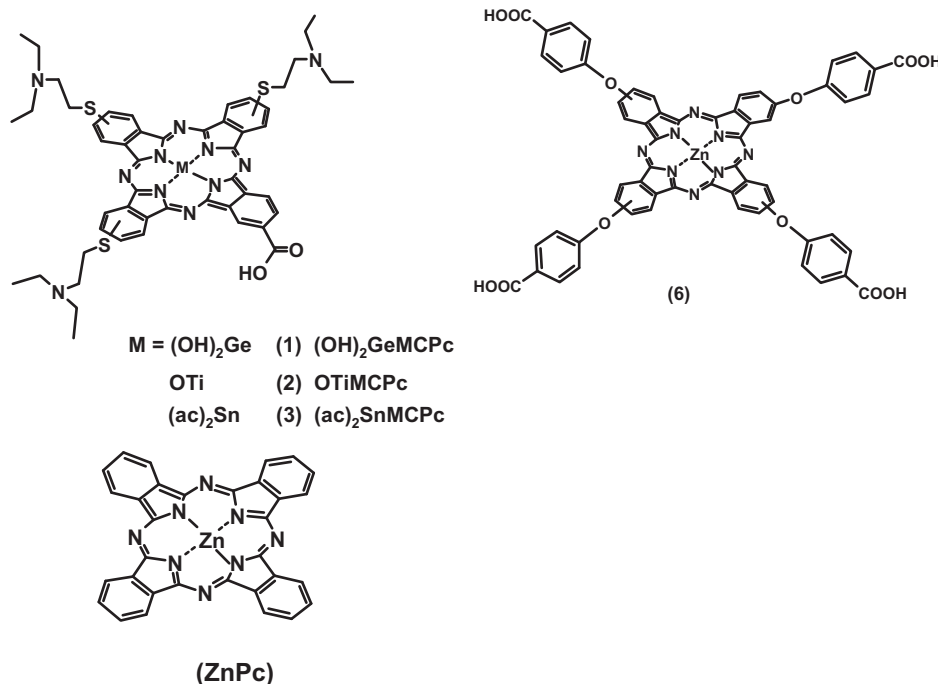


**Fig. 1.** Molecular structures of the low symmetrically substituted complexes. MCPc = monocarboxy phthalocyanine (complexes 1–3), TPCPc = tetraphenylcarboxyphthalocyanine (6) and ZnPc.

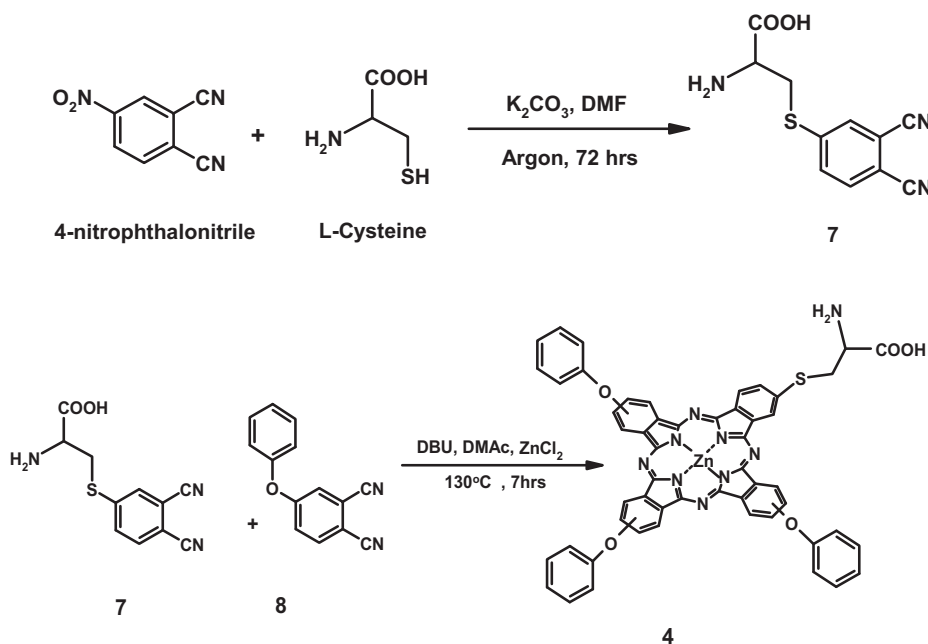
discussed. The results show that unsubstituted and symmetrically substituted ZnPc embedded in polystyrene are not active towards this bacteria due to low singlet oxygen production.

## 2. Experimental and methods

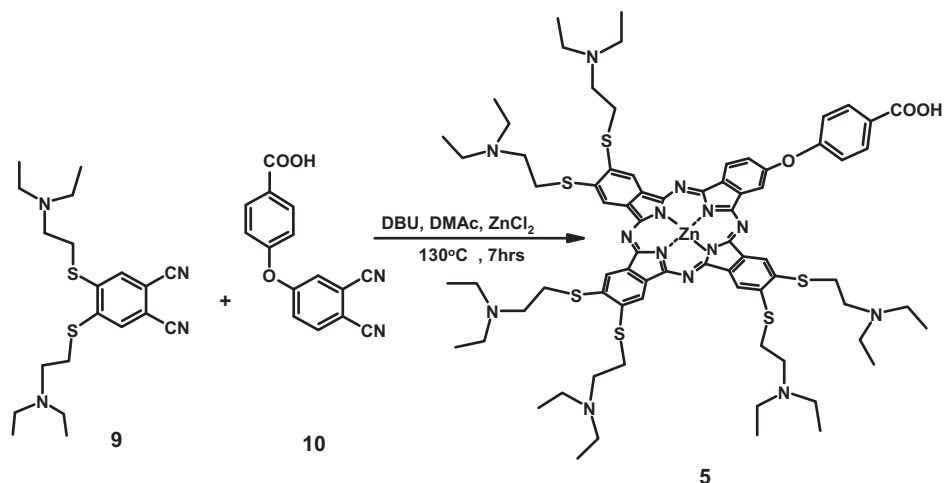
### 2.1. Materials

Polystyrene (PS, Mw = 192,000 g/mol), N,N-dimethylformamide (DMF), dimethylsulfoxide (DMSO), dichloromethane (DCM) and

tetrahydrofuran (THF) were from MERCK Chemical Ltd. Anthracene-9,10-bis-methylmalonate (ADMA), 1,3-diphenylisobenzofuran (DPBF), L-cysteine, dimethylacetamide (DMAc), 1,8-diazabicyclo [5.4.0]undec-7-ene (DBU), zinc chloride and zinc phthalocyanine (ZnPc) were purchased from Sigma–Aldrich. Agar bacteriological BBL Mueller Hinton broth and nutrient agar were purchased from Merck. *S. aureus* (ATCC 6538) was purchased from Microbiologics. The synthesis of complexes 1–3 [20] and 6 [21] (Fig. 1) have been reported in literature. Complexes 4 and 5 (Schemes 1 and 2) are reported here for the first time.



**Scheme 1.** Synthesis of 4-cysteinylnitrile (10) and low symmetry monocysteinylnitrile zinc (ZnMCsPc, 4).



**Scheme 2.** Synthesis of monophenoxy-carboxy zinc phthalocyanine (**ZnMPCPc**, **5**) complex.

## 2.2. Equipment

UV–visible spectra were recorded on a Shimadzu 2550 UV–Vis spectrophotometer. Fluorescence excitation and emission spectra were recorded on a Varian Eclipse spectrofluorometer. IR spectra (KBr pellets) were recorded on a Perkin–Elmer spectrum 2000 FTIR spectrometer.

Photo-irradiations for antimicrobial photo-inhibition studies and singlet oxygen determinations were performed using a General electric Quartz line lamp (300 W). A 600 nm glass cut off filter (Schott) and water were used to filter off ultraviolet and infrared radiations, respectively. An interference filter (Intor, 670 and 700 nm with a band width of 40 nm) was additionally placed in the light path before the sample. Light intensity was measured with a POWER MAX5100 (Molelectron detector incorporated) power meter. Scanning electron microscope (SEM) images of the fiber alone or in the presence of MPC complexes were obtained using a JOEL JSM 840 scanning electron microscope. The fiber diameters were measured using Cell-D software from Olympus. The average diameter of seventy different fibers was taken.

Mass spectral data were collected with a Bruker AutoFLEX III Smartbeam TOF/TOF Mass spectrometer. The spectra were acquired using dithranol as the MALDI matrix.

All plate readings for the antimicrobial studies were obtained using the LEDETECT 96 for in vitro diagnostic from LABXIM PRODUCTS.

## 2.3. Synthesis

4-Nitrophthalonitrile [22], 1,2 bis-(diethylaminoethylthiol)-4,5 dicyanobenzene (**9**) [23], 4-phenoxy phthalonitrile (**8**) [24] and 4-(3,4-dicyanophenoxy)benzoic acid (**10**) [25] were synthesized according to literature methods.

### 2.3.1. Synthesis of 4-cysteinyl phthalonitrile (**7**, Scheme 1)

Compound **7** was synthesized as follows: to dry DMF (30 mL) under argon, 3.5 g (25 mmol) of  $K_2CO_3$  was added. L-cysteine (2.07 g, 17.1 mmol) and 4-nitrophthalonitrile (2.0 g, 11.5 mmol) were added. After 4 and 24 h, more  $K_2CO_3$  (3.5 g, 25 mmol) was added to the mixture. The mixture was stirred at room temperature for 72 h, after this time the formed product was dissolved in water: methanol (1:1), and the pH of the solution adjusted to 2 by addition of HCl to give a light reddish brown precipitate. The product was further purified using size-exclusion column (Bio-Beads S-X1 from Bio-Rad).

Yield: 50%. IR [(KBr)-max/ $cm^{-1}$ ]: 3428 (OH), 3102 (C–H), 2234 (C≡N), 1610 (C=O), 1586, 1427, 1234, 862 (C–H), 742 (C–S–C). <sup>1</sup>H NMR (400 MHz, DMSO- $d_6$ )/ppm: 12.11 (1H, broad s, –COOH), 7.24 (1H, d, aromatic C–H), 7.56 (2H, dd, aromatic C–H), 3.89 (1H, d, C–H), 3.46 (2H, dd, S–CH<sub>2</sub>), 2.12 (2H, broad, NH<sub>2</sub>). Calc. for C<sub>11</sub> N<sub>3</sub>H<sub>9</sub>S<sub>1</sub>O<sub>2</sub>: C 53.46, H 3.64, N 17.00, S 12.97 Found: C 53.32, H 3.58, N 16.97, S 12.66.

### 2.3.2. Tris[9 (10), 16 (17), 23 (24)]-(4-phenoxy)-2-(4-cysteinyl) phthalocyanine} Zn (Scheme 1, (ZnMCsPc (**4**)))

A mixture of 4-cysteinyl phthalonitrile (**7**) (0.32 g, 1.3 mmol) and 4-phenoxy phthalonitrile (**8**) (0.86 g, 3.9 mmol) was firstly finely ground, homogenized and placed in a round bottom flask that contained pre-heated DMAc. The mixture was then stirred under reflux at 130 °C for 7 h in an argon atmosphere in the presence of excess zinc chloride as a metal salt and DBU as a catalyst. Thereafter, the mixture was cooled to room temperature and dropped in (1:1) water: acetone. The green solid product which precipitated was collected by centrifugation, washed with n-hexane and dried in air. Purification was achieved using column chromatography with silica gel as column material and MeOH (methanol):THF (2:10) as eluent followed by the addition of (2:1) THF:DMF to elute the second fraction which was our desired product. The product was dried in air and further washed with ethanol, acetone, n-hexane and diethyl ether.

Yield: (12.50%). IR (KBr,  $cm^{-1}$ ): 3452(O–H), 3128(C–H), 2977 (carboxylic acid OH), 1598 (C=O), 1534(C=C), 1447, 1348, 1300, 1235 (C–O–C) 878, 712 (C–S–C), 701,620, 553. NMR (DMSO- $d_6$ ):  $\delta$ , ppm 9.01–9.18 (12H, m, Pc–H), 7.27–7.88 (12H, m, aromatic-H), 7.10–7.21 (3H, dd, aromatic-H), 6.41–6.48 (1H, d, C–H), 4.53–4.59 (1H, br, OH) 3.62–3.71 (2H,d, S–CH<sub>2</sub>), 2.41–2.47 (2H, broad, NH<sub>2</sub>). UV/Vis (DMF)  $\lambda_{max}$  nm (log  $\epsilon$ ): 678 (5.09). Calc. for C<sub>53</sub> H<sub>33</sub> N<sub>9</sub> S<sub>1</sub> O<sub>5</sub> Zn: C 65.45, H 3.39, N 12.96, S 3.29 Found: C 64.98, H3.41, N13.01, S 3.13 MALDI TOF MS m/z: Calcd: 973.36 Found: [M – H]<sup>–</sup> = 972.82.

### 2.3.3. Hexakis [9; 10, 16; 17, 23; 24-(1,2-bis-(diethylaminoethylthiol))-2-(4-phenoxy-carboxy) phthalocyanine} Zn (Scheme 2, (ZnMPCPc (**5**)))

Synthesis for **5** was as outlined for **4** except 4-(3,4-dicyanophenoxy)benzoic acid (**10**) (0.34 g, 1.3 mmol) and 1,2-bis-(diethylaminoethanethiol)-4, 5-dicyanobenzene phthalonitrile (**9**) (1.52 g, 3.9 mmol) were employed instead of **7** and **8**. Purification was achieved using column chromatography with neutral alumina as column material and DCM:MeOH:THF (10:5:5) as eluent,

followed by drying. The desired product was further washed with ethanol, acetone, n-hexane and diethylether.

Yield: (15.10%). IR (KBr,  $\text{cm}^{-1}$ ): 3438(O–H), 3134(C–H), 2969 (carboxylic acid OH), 1610 (C=O) 1548(C=C), 1345, 1337, 1131, 854, 748 (C–S–C), 620, 553.  $^1\text{H}$  NMR (DMSO- $d_6$ ):  $\delta$ , ppm 10.01–10.09 (6H, m, Pc-H), 9.36–9.49 (3H, br, Pc-H), 7.35–7.23 (4H, m, aromatic), 4.63–4.71 (1H, br, OH), 3.25–3.30 (12H, m, S–CH<sub>2</sub>), 2.98–3.01 (12H, m, N–CH<sub>2</sub>), 2.56–2.71 (24H, m, CH<sub>2</sub>-methyl) 1.73–1.79 (36H, q, CH<sub>3</sub>). UV/Vis (DMF)  $\lambda_{\text{max}}$  nm (log  $\epsilon$ ): 695 (5.12). Calc. for C<sub>75</sub> H<sub>98</sub> N<sub>14</sub> S<sub>6</sub> O<sub>3</sub> Zn + H<sub>2</sub>O: C 59.31, H 6.45, N 12.91, S 12.67 Found: C 59.48, H 5.70, N 13.17, S 12.74. MALDI TOF MS  $m/z$ : Calcd: 1500.5 Found:  $[\text{M} + 2\text{H}]^{+2} = 1502.6$ .

#### 2.4. Preparation of electrospun nanofibers

The electrospinning technique (with or without MPC complexes) has been described before [26,27]. For the current work, the MPC:PS electrospun fibers were formed as follows: a solution containing  $1.3 \times 10^{-5}$  mol of polystyrene and  $1 \times 10^{-6}$  mol of MPC in 10 mL DMF/THF(4:1) was stirred for 24 h to produce a homogeneous solution. The solvent mixture of DMF/THF was employed to allow both the PS and MPC to dissolve. The solution was then placed in a cylindrical glass tube fitted with a capillary needle. A potential difference between anode and cathode of 20 kV (–5–15 kV) was applied to provide the charge for the spinning process. The distance between the cathode (static fiber collection point) and anode (tip of capillary needle) was 15 cm. The pump rate was maintained at 0.5 mL/h. The flow rate was increased to 1 mL/h in the case of the polystyrene/phthalocyanine composite to avoid clogging of the needle.

#### 2.5. Antimicrobial activity

*S. aureus* (*S. aureus*) was grown on a nutrient agar plate prepared according to the manufacturer's specifications. Electrospun fibers modified with phthalocyanines were placed on the Baird Parker agar base plates which were pre-inoculated with 100  $\mu\text{L}$  of liquid broth containing a suspension of *S. aureus* ( $\sim 10^7$ – $10^8$  CFU/mL (colony forming unit/mL)). This resulted in bacteria growing over and around the fiber, hence completely covering it. One pair of agar plates was kept in the dark for 90 min and the other pair was kept under illumination with visible light (as described in Section 2.2) for 90 min. All the samples were incubated for 16 h at 37 °C. A pair of agar plates containing the PS/Pc fiber without bacteria was used as control both in the dark and under illumination with light. This was aimed at confirming that the changes observed are due to bacteria inactivation and not phthalocyanine leaching, even though the latter is not expected due to insolubility of the complexes in water.

The antimicrobial activity of the MPCs was also studied in solution (not using a fiber mat). Firstly, single colony of *S. aureus* from the agar plate was inoculated into 10 mL of Mueller Hinton nutrient broth and allowed to grow at 37 °C for 2–6 h until an appropriate optical density (0.6–0.8 at 600 nm) was obtained. Separately, MPCs solutions (100  $\mu\text{L}$  with concentrations ranging from 0.16 to 20  $\mu\text{M}$  in DMF) were added to the 96 well plates containing 100  $\mu\text{L}$  Mueller Hinton nutrient broth. Then, 5  $\mu\text{L}$  of the solution of *S. aureus* prepared on the first step was pipetted into each 96 well plates containing the MPCs. The total amount of DMF in each well was 50%. *S. aureus* is known to be resistant to DMF [28].

A pair of 96 wells microplate containing the same Pc molecule was then irradiated with visible light for 90 min, while another pair was kept in the dark. Irradiated and non-irradiated cells were incubated overnight on an incubator shaker ( $\sim 200$  rpm) in the

dark at 37 °C. The viable microorganisms were corrected with controls containing no Pc. The optical density of the bacterial viability was determined at 600 nm and expressed as percentage growth inhibition. The experiments were done in triplicates.

#### 2.6. Singlet oxygen quantum yield

Singlet oxygen quantum yield ( $\Phi_{\Delta}$ ) values were determined in air using the relative method with DPBF acting as a singlet oxygen chemical quencher in DMF. Equation (1) was employed for calculating singlet oxygen quantum yields:

$$\Phi_{\Delta} = \Phi_{\Delta}^{\text{Std}} \cdot \frac{R I_{\text{abs}}^{\text{Std}}}{R^{\text{Std}} I_{\text{abs}}} \quad (1)$$

where  $\Phi_{\Delta}^{\text{Std}}$  is the singlet oxygen quantum yield for the standard (ZnPc,  $\Phi_{\Delta}^{\text{Std}} = 0.56$  in DMF) [29].  $R$  and  $R^{\text{Std}}$  are the DPBF photobleaching rates in the presence of the metallophthalocyanine derivatives under investigation and the standard respectively.  $I_{\text{abs}}$  and  $I_{\text{abs}}^{\text{Std}}$  are the rates of light absorption by the MPC derivatives and the standard, respectively. To avoid chain reactions of the quencher in the presence of singlet oxygen [29], the concentration of DPBF was kept at  $\sim 3 \times 10^{-5}$  mol L<sup>-1</sup>.

Solutions of the MPCs with an absorbance of  $\sim 0.5$  at the irradiation wavelength were prepared in the dark and irradiated at the Q band region in the presence of DPBF. The DPBF absorption at 417 nm was monitored with photolysis time. The error was  $\sim 10\%$  from several values of  $\Phi_{\Delta}$ .

For the modified fibers the absolute method was used. The singlet oxygen quantum yield ( $\Phi_{\Delta}$ ) determinations for the MPC on fibers were carried out in aqueous solutions using ADMA as the quencher and its degradation was monitored at 380 nm. In each case 10 mg of the modified fibers was suspended (as small pieces) in an aqueous solution of ADMA and irradiated using the photolysis set-up described above. The quantum yields ( $\Phi_{\text{ADMA}}$ ) were calculated using equation (2), using the extinction coefficient of ADMA in water, log ( $\epsilon$ ) = 4.1 [30].

$$\Phi_{\text{ADMA}} = \frac{(C_0 - C_t)V_R}{I_{\text{abs}} \cdot t} \quad (2)$$

where  $C_0$  and  $C_t$  are the ADMA concentrations prior to and after irradiation, respectively;  $V_R$  is the solution volume;  $t$  is the irradiation time per cycle and  $I_{\text{abs}}$  is defined by equation (3).

$$I_{\text{abs}} = \frac{\alpha \cdot A \cdot I}{N_A} \quad (3)$$

where  $\alpha = 1 - 10^{-A(\lambda)}$ ,  $A(\lambda)$  is the absorbance of the sensitizer at the irradiation wavelength,  $A$  is the irradiated area (2.5 cm<sup>2</sup>),  $I$  is the intensity of light ( $4.54 \times 10^{16}$  photons cm<sup>-2</sup> s<sup>-1</sup>) and  $N_A$  is Avogadro's constant.

The absorbances used for equation (3) are those of the phthalocyanines in the fibers (not in solution) measured by placing the modified fiber directly on a glass plate. The light intensity measured refers to the light reaching the spectrophotometer cells, and it is expected that some of the light may be scattered, hence the  $\Phi_{\Delta}$  values of the phthalocyanines in the fiber are estimates. The singlet oxygen quantum yields ( $\Phi_{\Delta}$ ) were calculated using equation (4) [31]

$$\frac{1}{\Phi_{\text{ADMA}}} = \frac{1}{\Phi_{\Delta}} + \frac{1}{\Phi_{\Delta}} \cdot \frac{k_d}{k_a} \cdot \frac{1}{[\text{ADMA}]} \quad (4)$$

where  $k_d$  is the decay constant of singlet oxygen in respective solvent and  $k_a$  is the rate constant of the reaction of ADMA with

$O_2(^1\Delta_g)$ . The intercept obtained from the plot of  $1/\Phi_{ADMA}$  versus  $1/[ADMA]$  gives  $1/\Phi_{\Delta}$ .

### 3. Results and discussion

#### 3.1. Spectroscopic and microscopic characterization

The MPC complexes were mixed with polystyrene and electrospun into nanofibers as explained in the experimental section. Scanning electron microscope images of the various MPC complexes incorporated into polystyrene, Fig. 2 shows highly branched cylindrical network of nanofibers. The fiber diameter ranged from  $240 \pm 45$  nm to  $390 \pm 30$  nm, Table 1. The polystyrene alone gave the smallest fiber diameter average of  $240 \pm 45$  nm which is within the range of previously reported average diameter of polystyrene [32]. An increase in fiber diameter was obtained in the presence of phthalocyanines. The ZnMPCPc-PS composite gave the highest average fiber diameter of  $390 \pm 30$  nm compared to all the other complexes, followed by  $(ac)_2SnMPCPc$  with the average diameter of  $370 \pm 30$  nm respectively, Table 1. The solution properties such viscosity, conductivity and surface tension may affect the fiber formation hence the diameter of the fibers. Differences and the conductivities of MPC complexes may have a large effect on the electrospinning process. Differences in the nature of the central metal atom, inter-planar distances between the molecules and differences in stacking arrangements of the molecules all affect conductivity in phthalocyanines [33], hence fiber diameter.

The UV–visible absorption spectra of the complexes in solution and in the polymer support are shown in Fig. 3. Blue shift in the Q band spectra was observed for  $(OH)_2GeMPCPc$  (1), OTiMPCPc (2),

**Table 1**

Spectral, microscopic and photochemical properties of the low symmetry MPC complexes in solution (DMF) and in the fiber matrix (water).

Sample	$\lambda_Q$ /nm (solution)	$\lambda_Q$ /nm (solid)	$\Phi_{\Delta}$ (solution)	$\Phi_{\Delta}$ (fiber)	Average diameter (nm)
$(OH)_2GeMPCPc$ (1)	695	692	0.66	0.46	$275 \pm 30$
OTiMPCPc (2)	734	728	0.54	0.31	$315 \pm 30$
$(ac)_2SnMPCPc$ (3)	720	716	0.52	0.30	$370 \pm 30$
ZnMCSpc (4)	678	680	0.57	0.42	$260 \pm 30$
ZnMPCPc (5) <sup>a</sup>	695 (683)	684 (680)	0.64 (0.45)	0.28 (0.12)	$390 \pm 30$
ZnPc	670	668	0.56	0.14	$305 \pm 35$
Polystyrene	–	–	–	–	$240 \pm 45$

<sup>a</sup> Numbers in brackets are for the symmetrical ZnTPCPC(6).

$(ac)_2SnMPCPc$  (3) and ZnMPCPc(5) on the fiber (curves ii in Fig. 3). The blue shifting in the spectra of these complexes, which contain sulfur bridges, suggests that there is interaction of the fiber with the S groups, since S groups are known to result in red shifting. For ZnTPCPC (6) containing no S groups there was no blue shifting but broadening due to aggregation. Broadening in spectra was also observed for ZnMPCPc (5).  $(ac)_2SnMPCPc$  (3) showed a clear split in the Q band with the high energy band being due to the aggregate and the low energy band due to the monomer. Aggregation of phthalocyanines in general is expected in the solid state due to the close proximity of Pc–Pc rings, which results in very strong  $\pi$ – $\pi$  interactions. The  $(OH)_2GeMPCPc$  (1) and ZnMCSpc (4) complexes did not show aggregation on the polymer fiber. ZnMCSpc (4) showed a slight red shift in the solid state as opposed to blue shifting. Red shifting of phthalocyanine Q-band in the polymer fiber has been reported before [19].

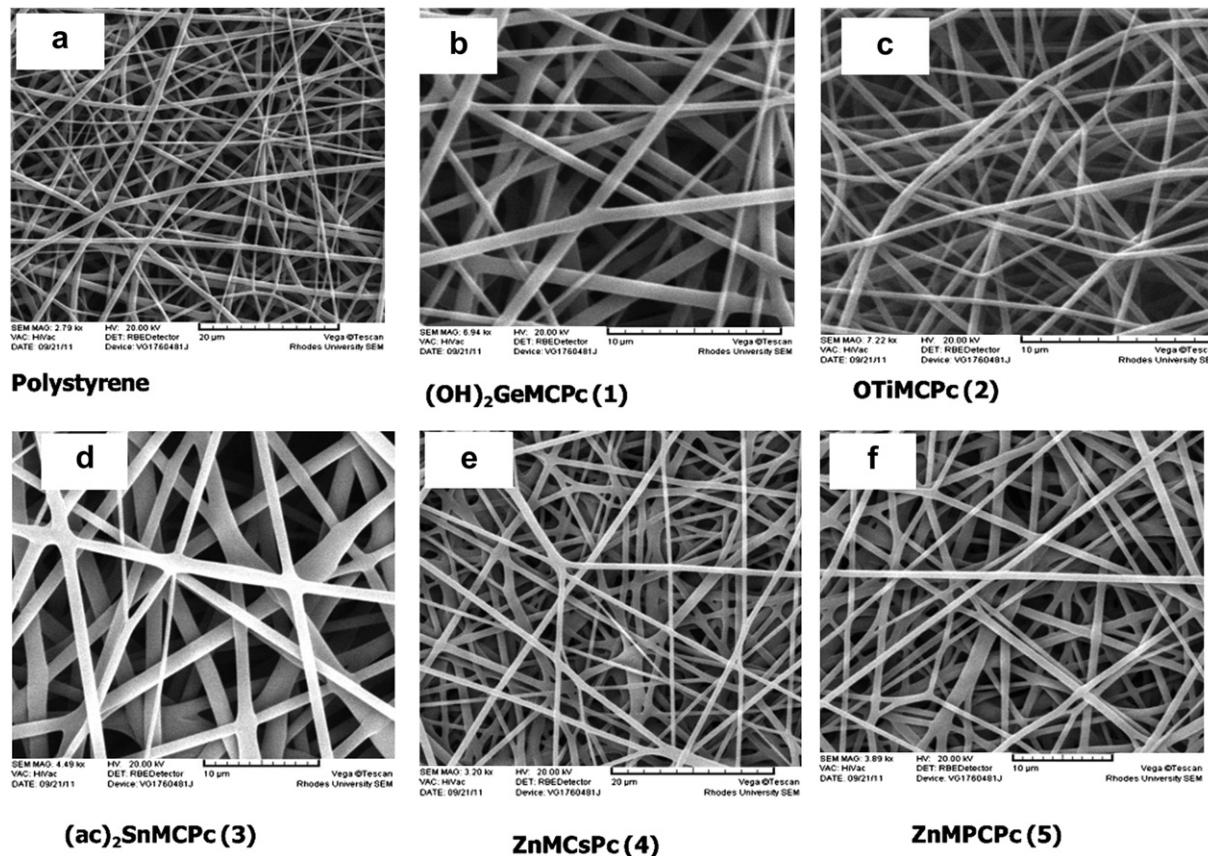


**Fig. 2.** Scanning electron microscopic (SEM) images polystyrene electrospun fiber alone (a),  $(OH)_2GeMPCPc$  (1):PS (b), OTiMPCPc (2):PS (c),  $(ac)_2SnMPCPc$  (3):PS (d), ZnMCSpc (4):PS (e) and ZnMPCPc (5):PS (f), and. Scale = 10  $\mu$ m.

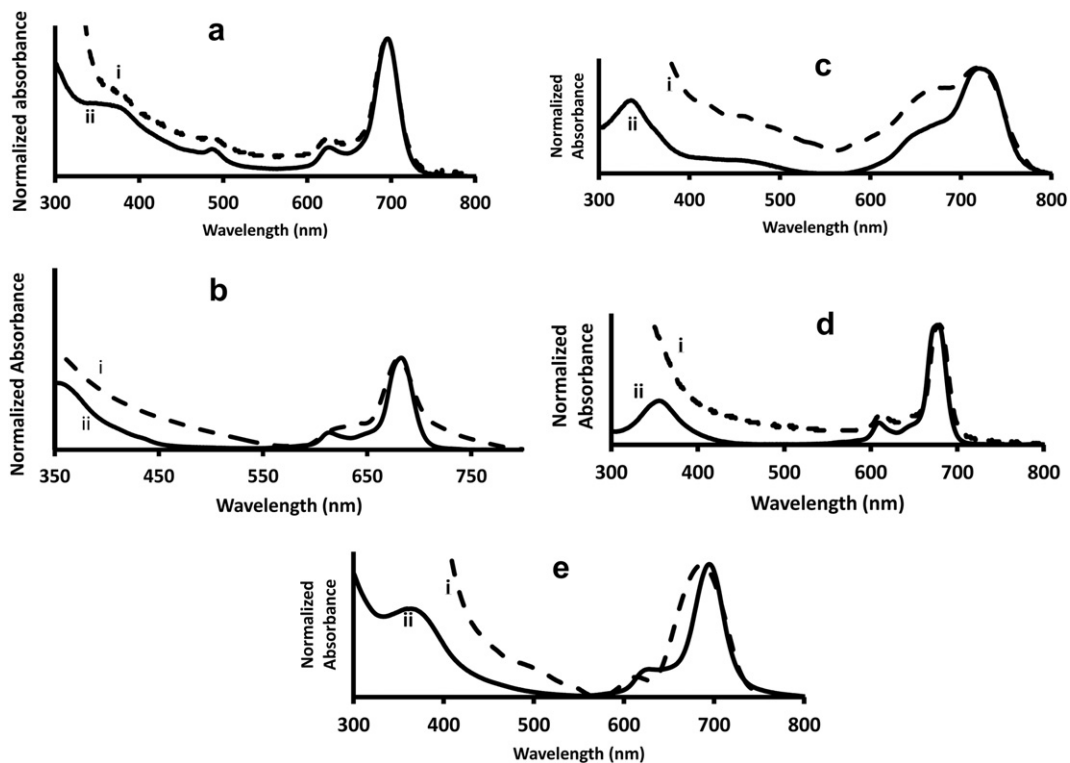


**Fig. 3.** Ground state electronic absorption spectra of (a)  $(\text{OH})_2\text{GeMCPc}$  (**1**), (b)  $\text{OTiMCPc}$  (**2**), (c)  $(\text{ac})_2\text{SnMCPc}$  (**3**), (d)  $\text{ZnMCPc}$  (**4**) and (e)  $\text{ZnMPCPc}$  (**5**), in (dotted line) (polymer fiber) and in solution (solid line) (DMF).

The IR spectra of polystyrene shows characteristic signals in the aromatic finger print region which are due to the styrene subunits (Fig. 4(ii)). The aromatic  $\text{C}=\text{C}$  bend from the styrene ring is observed at the region  $\sim 1470\text{--}1600\text{ cm}^{-1}$ . An increase in the intensity of aromatic signals in the  $1470\text{--}1600\text{ cm}^{-1}$  was observed on the IR spectra of MPC-PS composite (using  $(\text{ac})_2\text{SnMCPc}$  (**3**) as an example) suggesting additional aromatic rings from the Pc ring (Fig. 4(i)). The intense carbonyl  $\text{C}=\text{O}$  stretching around  $\sim 1650\text{ cm}^{-1}$  was observed for all the complexes, and is due to the carboxylic acid groups of the phthalocyanine complexes, serving as a further confirmation of the presence of Pc in the polymer fiber.

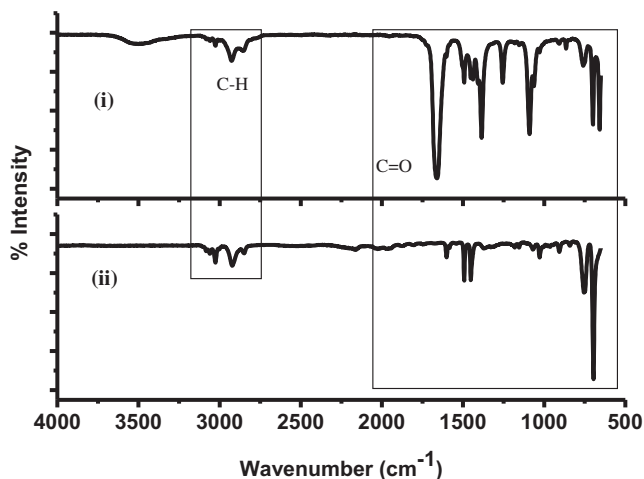


**Fig. 4.** Infrared spectra of  $(\text{ac})_2\text{SnMCPc}$ (**3**)/PS (i) and polystyrene fiber alone (ii).

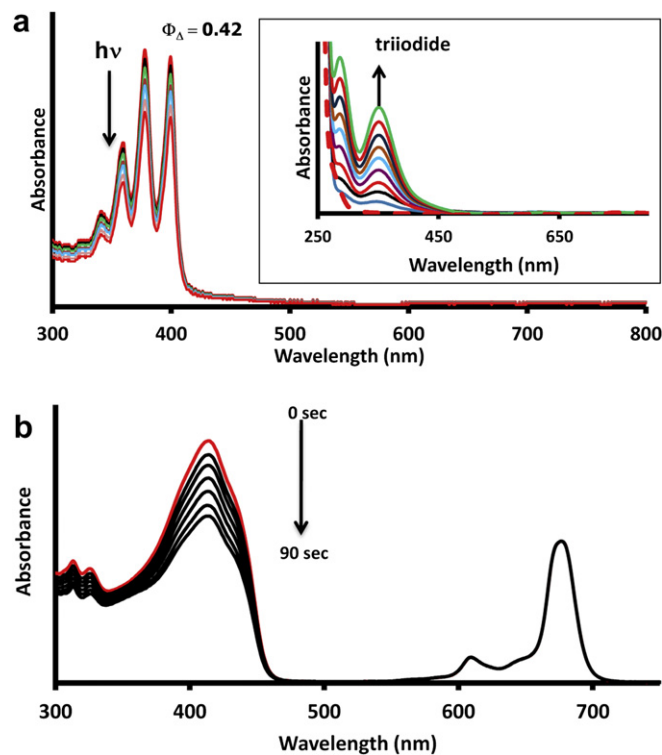


**Fig. 5.** Photodegradation of ADMA in the presence of  $\text{ZnMCPc}$  (**4**):PS fiber (a) and photodegradation of DPBF in the presence of  $\text{ZnMCPc}$  (**4**) in DMF (b). Inset: Photo-oxidative generation of triiodide in the presence  $\text{ZnMCPc}$  (**4**) in aqueous media.

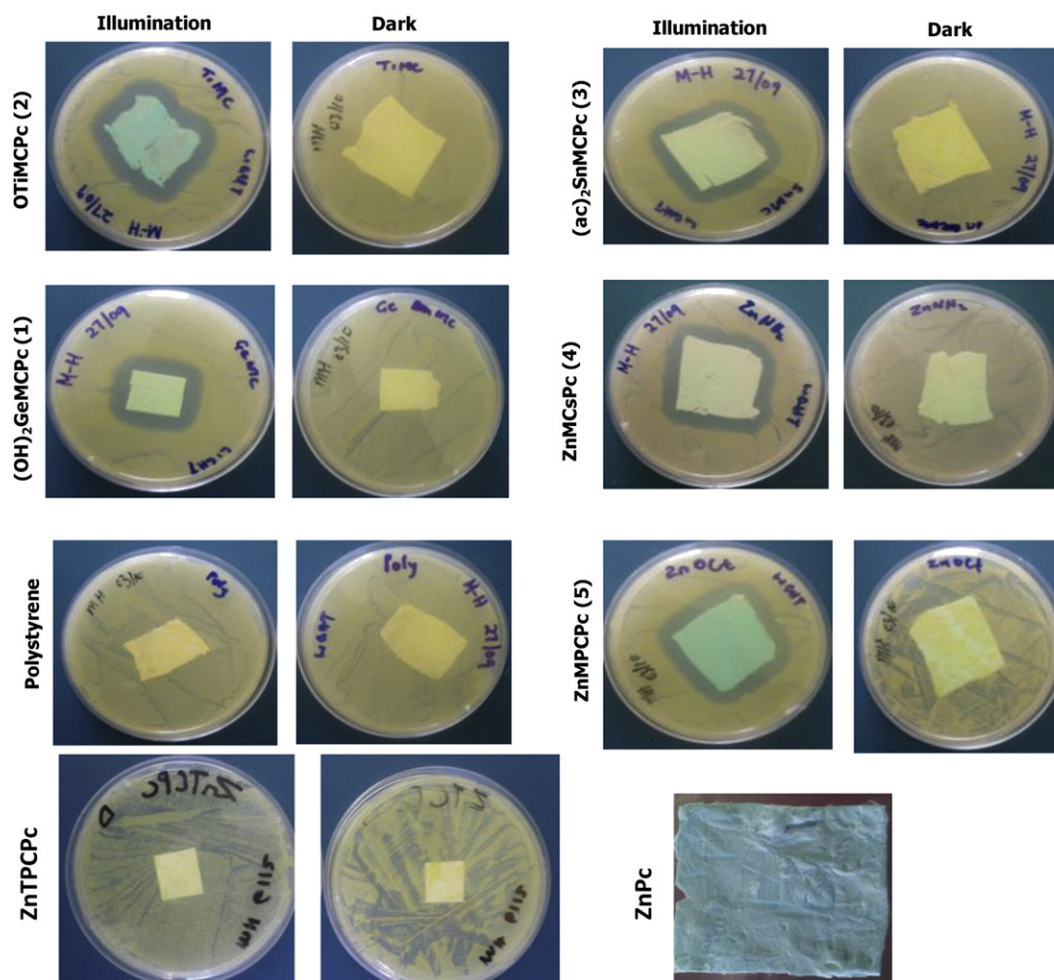


Fig. 6. Images of the antimicrobial inhibition test using phthalocyanine modified fibers, studies in the dark and under illumination with visible light. Unmodified polystyrene alone employed as a control. The figure also shows PS/ZnPc fiber before use in agar plate for bacterial growth.

### 3.2. Singlet oxygen generating abilities of the MPc in solution and on fiber

The ability of a photosensitizer to absorb light and produce a cytotoxic singlet oxygen species serve as a selective tool for photodynamic therapeutic applications. The singlet oxygen quantum yields ( $\Phi_{\Delta}$ ) were determined by monitoring the photo-degradation of ADMA (in aqueous solution for the fiber matrix (Fig. 5(a))) and DPBF (in DMF for the MPc complexes (Fig. 5(b))), using ZnMCPc (4) complex as an example. Complimentary to the degradation of ADMA, the polymer composite consisting of the MPcs was used for the generation of triiodide ( $I_3^-$ ) from iodide ( $I^-$ ) in the presence of light as observed in Fig. 5(a) (insert), serving as a clear proof that singlet oxygen is produced as the  $I_3^-$  absorption band increase with time [34]. There was no absorption in the region between 600 and 800 nm (Fig. 5(a)) where the main absorption band of the phthalocyanine is located, suggesting no leakage of phthalocyanines from the fiber to the solution in aqueous media. This is expected since the phthalocyanines reported in this work are not soluble in water. The lack of leaching in water is important for real biological applications of the fibers in aqueous media as is the case in this work.

As stated in the introduction, metallophthalocyanines containing diamagnetic metals exhibit high photosensitizing abilities [35–37], which enhance their singlet oxygen generation, hence are employed in this work. In addition, some of the central metals used in this work such as Ge (IV), Sn (IV) and Ti (IV) carry axial ligands

that can help minimize aggregation. Aggregation has been reported to lower the triplet state behavior resulting in low singlet oxygen quantum yields [35,36].

Higher singlet oxygen quantum yields were obtained for the complexes in solution compared to fiber matrix (Table 1). The decrease in the values of  $\Phi_{\Delta}$  in the solid state might due to aggregation in some cases. The  $(OH)_2GeMCPc$  (1) complex gave the highest ( $\Phi_{\Delta}$ ) value of 0.66 and 0.46 both in solution and in the fiber matrix. In the fiber, ZnMCPc (4) gave the second highest value of  $\Phi_{\Delta} = 0.42$  in the fiber. Higher  $\Phi_{\Delta}$  values for the ZnMCPc (4) and the  $(OH)_2GeMCPc$  (1) complexes in fiber may have been a result of the less aggregation behavior of these complexes in the solid state, as was discussed above for the UV–Vis spectra. Of the asymmetrical Pc complexes, ZnMPCPc (5) gave the lowest singlet oxygen value of 0.28 in the fiber matrix. The singlet oxygen quantum yield production of low symmetry phthalocyanines in the solid stage (fiber) are reported for the first time. Symmetrically substituted ZnTPCPC (6) and unsubstituted ZnPc showed the lowest  $\Phi_{\Delta}$  values of all complexes both in solution and when embedded in the fiber, Table 1. ZnTPCPC (6) gave lower  $\Phi_{\Delta}$  values than ZnMPCPc (5), the latter is the unsymmetrical tetrasubstituted derivative of former.

### 3.3. Photo-inhibition of *S. aureus*

The mechanism and the science behind photodynamic antimicrobial chemotherapy (PACT) is in its infancy, but it seems to follow

the same mechanism and principles as PDT and hence involves singlet oxygen. It is known that singlet oxygen reacts with intercellular molecules (peptides and proteins etc) leading to oxidative damage of the cell wall and cell membrane which cause cell death [7]. A series of low symmetry phthalocyanines presented in this study shows photo-activity in the presence of light hence their PACT was investigated.

The photodynamic responses of the complexes were investigated in the fiber matrix. Fig. 6 shows digital images of the nutrient agar plates containing *S. aureus* in contact with electrospun fibers. The Pcs embedded in the fiber are blue in color in the absence of bacteria (in nutrient broth or as a separate fiber, Fig. 6, ZnPc as an example). The bacteria grew on and around the fiber resulting in the blue color of the Pcs on the fiber disappearing. The samples irradiated with light in the presence of bacteria showed positive growth inhibition as compared to those that were kept in the dark. This is judged by the clearing around the fiber and the restoration of the blue color of the fiber. The polystyrene fiber alone did not show any bacterial inhibition both in the dark and under illumination with light. Lack of growth of bacteria around the polymer fiber modified with photosensitizers (Fig. 6) was obtained for all low symmetry MPC complexes as a result of bacterial growth inhibition. This serves as evidence that the monocarboxy phthalocyanine complexes generate reactive oxygen species that prevent bacterial growth.

A pair of plates containing a nutrient agar with polymer fiber in the absence of bacteria was used as a control both in the dark and under illumination with light. The color of the Pc modified fiber was blue both under illumination and in the dark (control images not shown). The nutrient agar was prepared in aqueous media and Pcs are insoluble in aqueous media, hence there was no possible leaching or migration of phthalocyanine from the fiber matrix to the nutrient agar from the control experiments both in the presence and in the absence of bacteria.

The symmetrical ZnTPCPc (**6**) (Fig. 6) and ZnPc showed no activity towards bacterial inactivation most likely due to the low

singlet oxygen quantum yield value. Thus even though unsubstituted ZnPc embedded in electrospun fiber was reported to show inactivation of *E. coli* [19], its low singlet oxygen quantum yield resulted in no activity for the more drug resistant *S. Aureus*. This confirms the importance of reasonably large values of singlet oxygen quantum yields for successful bacterial inactivation. The lack of activity of the symmetrical ZnTPCPc (**6**), shows the importance of unsymmetrical substitution with the carboxyphenoxy substituent.

The photo-inhibition studies were also investigated for all the complexes in solution, as shown in Fig. 7. The minimum inhibitory concentration (MIC) required to inhibit 50% bacterial growth was used as a reference to determine the effectiveness of these promising antimicrobials photosensitizers towards the inactivation of *S. aureus*. The minimum concentration of  $\sim 10 \mu\text{M}$  at which approximately  $\sim 50\%$  bacterial inhibition was obtained for all the MPC samples when kept in the dark, Fig. 7(a). A significant improvement in bacterial inhibition was obtained for the samples illuminated with light (Fig. 7(b)) giving  $\sim 50\%$  of bacterial inhibition at a much lower concentration of  $\sim 1.25 \mu\text{M}$ . This suggested that the production of singlet oxygen had a strong contribution in photo-inhibition of bacteria.

With the results presented in this work, the phthalocyanine complexes studied showed a potential industrial application for antimicrobial photo-inhibition of *S. aureus*.

#### 4. Conclusions

The photochemical behavior of a series of low symmetry phthalocyanine complexes has been investigated. All the MPC complexes showed the production of singlet oxygen both in the fiber matrix and in solution. We report for the first time the antimicrobial photo-inhibition activities of a series of low symmetry phthalocyanine complexes supported on a polymer fiber and compare the activity with symmetrically and unsubstituted ZnPc. The study shows positive results that can be further engineered for industrial applications. Lack of bacterial growth was observed on areas surrounding the modified fiber, confirming successful bacterial growth inhibition. The minimum inhibition concentration results showed  $\sim 50\%$  of the bacterial inhibition at  $\sim 1.25 \mu\text{M}$  MPC concentration in DMF:broth mixture.

#### Acknowledgments

This work was supported by the Department of Science and Technology (DST) and National Research Foundation (NRF) of South Africa through DST/NRF South African Research Chairs Initiative for Professor of Medicinal Chemistry and Nanotechnology and Rhodes University. The project was partially funded by FP7-PEOPLE-2009-IRSES PROCOTEX.

#### References

- [1] Gregory P. High-technology applications of organic colourant. New York: Plenum Press; 1991. p. 7–273.
- [2] McKeown NB. Phthalocyanine materials: synthesis, structure and function. Chemistry of solid state materials. New York: Cambridge University Press; 1998. p. 32–149.
- [3] Nombona N, Maduray K, Antunes E, Karsten A, Nyokong T. Synthesis of phthalocyanine conjugates with gold nanoparticles and liposomes for photodynamic therapy. J Photochem Photobiol B: Biol 2012;107:35–44.
- [4] Bonnett R, editor. Chemical aspects of photodynamic therapy. The Netherlands, Amsteldijk: Gordon and Breach Science; 2000. pp. 199–222.
- [5] Jiang X-J, Yeung S-L, Lo P-C, Fong W-P, P Ng DK. J Med Chem 2011;54:320.
- [6] Pandey RK, Zheng G. In: Kadish KM, Smith KM, Guillard R, editors. Porphyrins as photosensitizers in photodynamic therapy. The porphyrin handbook, vol. 6. San Diego: Academic Press; 2000 [Chapter 43].
- [7] Dougherty TJ, Gomer CJ, Henderson BW, Jori G, Kessel D, Korbek M, et al. J Natl Cancer Inst 1998;90:889.

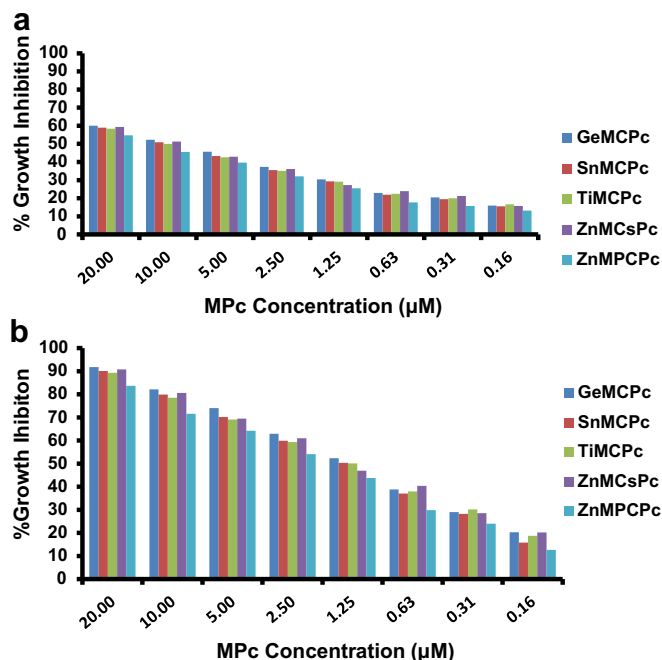


Fig. 7. Antimicrobial activity of the MPC complexes in liquid broth solution, in the dark (a) and under illumination with visible light (b).

- [8] Jori G, Fabris C, Soncin M, Ferro S, Coppelotti O, Dei D, et al. Photodynamic therapy in the treatment of microbial infections: basic principles and perspective applications. *Lasers Surg Med* 2006;38:468–81.
- [9] Wainwright M. Photodynamic antimicrobial chemotherapy (PACT). *J Antimicrob Chemother* 1998;42:13–28.
- [10] Chen J, Chen Z, Zheng Y, Zhou S, Wang J, Chen N, et al. Substituted zinc phthalocyanine as an antimicrobial photosensitizer for periodontitis treatment. *J Porphyr Phthalocya* 2011;15:293–9.
- [11] Kasuga H. In: Lever APB, Leznoff CC, editors. Phthalocyanine: properties and applications, vol. 4. New York: VCH Publishers; 1996.
- [12] Nyokong T, Antunes E [Chap. 34]. In: Kadish KM, Smith KM, Guillard R, editors. The handbook of porphyrin science, vol. 7. New York: Academic Press; 2010. p. 247–349 [World Scientific, Singapore].
- [13] Masilela N, Nyokong T. The synthesis and photophysical properties of novel cationic tetra pyridiloxo substituted aluminium, silicon and titanium phthalocyanines in water. *J Lumin* 2010;130:1787–93.
- [14] Durmus M, Nyokong T. Synthesis, photophysical and photochemical properties of aryloxy tetra-substituted gallium and indium phthalocyanine derivatives. *Tetrahedron* 2007;63:1385–94.
- [15] Masilela N, Nombona N, Loewenstein T, Nyokong T, Schlettwein D. Symmetrically and unsymmetrically substituted carboxy phthalocyanines as sensitizers for nanoporous ZnO films. *J Porphyr Phthalocya* 2010;14:985–92.
- [16] Weitemeyer A, Kleish H, Michelsen U, Hirtb A, Wöhrle D. In: Moser JG, editor. Photodynamic tumor therapy: 2nd and 3rd generation photosensitizers. The Netherlands: Harwood Academic Publishers [Chpt. 2], [http://www.routledge.com/9789056991395&usg=AFQjCNHE4GG5SejdljUcTB9nqVNsBIA5wA&source=gs\\_buy\\_r](http://books.google.co.za/url?client=ca-print-tandf_uk-taylor_francis&format=googleprint&num=0&channel=BTB-ca-print-tandf_uk-taylor_francis+BTB-ISBN:9056991396&q=http://www.routledge.com/9789056991395&usg=AFQjCNHE4GG5SejdljUcTB9nqVNsBIA5wA&source=gs_buy_r); 1998.
- [17] Cosimelli B, Roncucci G, Dei D, Fantetti L, Ferroni F, Riccio M, et al. Synthesis and antimicrobial activity of new unsymmetrical substituted zinc phthalocyanines. *Tetrahedron* 2003;59:10025–30.
- [18] Nombona N, Antunes E, Chidawanyika W, Kleyi P, Tshentu Z, Nyokong T. Synthesis, photophysics and photochemistry of phthalocyanine- $\epsilon$ -polylysine conjugates in the presence of metal nanoparticles against *Staphylococcus aureus*. *J Photochem Photobiol A: Chem* 2012;233:24–33.
- [19] Mosinger J, Lang K, Kubát P, Sýkora J, Hof M, Plíštil L, et al. Photofunctional polyurethane nanofabrics doped by zinc tetraphenyl porphyrin and zinc phthalocyanine photosensitizers. *J Fluoresc* 2009;19:705–13.
- [20] Masilela N, Nyokong T. The synthesis and fluorescence behaviour of new unsymmetrically mono-functionalized carboxy Ge, Ti and phthalocyanines. *Dyes Pigments* 2011;91:164–9.
- [21] Nazeeruddin Md K, Humphry-Baker R, Grätzel M, Wöhrle D, Schnurpfeil G, Schneider G, et al. Efficient near-IR sensitization of nanocrystalline TiO<sub>2</sub> films by zinc and aluminum phthalocyanines. *J Porphyr Phthalocya* 1999;3:230–7.
- [22] Wöhrle D, Eskes M, Shigehara K, Yamada A. A simple synthesis of 4,5-disubstituted 1,2-dicyanobenzenes and 2,3,9,10,16,17,23,24-octasubstituted phthalocyanines. *Synthesis* 1993:194–6.
- [23] Bayir ZA. Synthesis and characterization of novel soluble octa-cationic phthalocyanines. *Dyes Pigments* 2005;65:235–42.
- [24] Tau P, Nyokong T. Synthesis and electrochemical characterisation of  $\alpha$ - and  $\beta$ -tetra-substituted oxo (phthalocyaninato) titanium(IV) complexes. *Polyhedron* 2006;25:1802–10.
- [25] Chidawanyika W, Nyokong T. The synthesis and photophysicochemical properties of low-symmetry zinc phthalocyanine analogues. *J Photochem Photobiol A: Chem* 2009;206:169–76.
- [26] Tang S, Shao C, Liu Y, Li S, Mu R. Electrospun nanofibers of poly(ethylene oxide)/teraamino phthalocyanine copper(II) hybrids and its photoluminescence properties. *J Phys Chem Solids* 2007;68:2337–40.
- [27] Li D, Xia YN. Electrospinning of nanofibers: reinventing the wheel? *Adv Mater* 2004;16:1151–70.
- [28] Barry AL, Lasner RA. Inhibition of bacterial growth by the nitrofurantoin solvent dimethylformamide. *Antimicrob Agents Chemother* 1976;9:549–50.
- [29] Spiller W, Kliesch H, Worhle D, Hackbarth S, Roder B, Schnurpfeil G. Singlet oxygen quantum yields of different photosensitizers in polar solvents and micellar solution. *J Porphyr Phthalocya* 1998;2:145–58.
- [30] Ogunsipe A, Nyokong T. Photophysical and photochemical studies of sulfonated non-transition metal phthalocyanines in aqueous and non-aqueous media. *J Photochem Photobiol A* 2005;173:211–20.
- [31] Foote CS. Quenching of singlet oxygen. In: Wasserman HH, Murray RW, editors. singlet oxygen. New York, San Francisco, London: Academic Press; 1979. p. 139–71.
- [32] Zugle R, Antunes E, Khene S, Nyokong T. Photooxidation of 4-chlorophenol sensitized by lutetium tetraphenoxy phthalocyanine anchored on electrospun polystyrene polymer fiber. *Polyhedron* 2012;33:74–81.
- [33] Achar BN, Lokesh KS. Studies on tetra-amine phthalocyanines. *J Organomet Chem* 2004;689:3357–61.
- [34] Cerny J, Karaskova M, Rakusan J, Nespurek S. Reactive oxygen species produced by irradiation of some phthalocyanine derivatives. *J Photochem Photobiol A: Chem* 2010;210:82–8.
- [35] Idowu M, Nyokong T. Synthesis, photophysics and photochemistry of tin(IV)phthalocyaninederivatives. *J Photochem Photobiol A: Chem* 2008; 199:282–90.
- [36] Idowu M, Nyokong T. Photosensitizing properties of octacarboxymetallophthalocyanines in aqueous medium and their interaction with bovine serum albumin. *J Photochem Photobiol A: Chem* 2008;200:396–401.
- [37] Arslanoglu Y, Idowua M, Nyokong T. Synthesis and photophysical properties of peripherally and non-peripherally mercaptopyrindine substituted metal free, Mg(II) and Al(III) phthalocyanines. *Spectrochim Acta Part A: Mol Biomol Spectrosc* 2012;95:407–13.